ELSEVIER

Journal of Alloys and Compounds 448 (2008) 308–312

Journal of ALLOYS AND COMPOUNDS

www.elsevier.com/locate/jallcom

Thermoelectric properties of p-type Te-doped $(Bi,Sb)_2Te_3$ alloys by mechanical alloying and plasma activated sintering

Xi'an Fan, Junyou Yang *, Wen Zhu, Siqian Bao, Xingkai Duan, Qinqin Zhang

State Key Laboratory of Materials Processing and Dies & Mould Technology, Huazhong University of Science and Technology, 1037 Luoyu Road, Wuhan 430074, PR China

Received 30 September 2006; received in revised form 12 October 2006; accepted 16 October 2006
Available online 21 November 2006

Abstract

In the present work, p-type $(Bi,Sb)_2Te_3$ alloys with excess Te addition were prepared by mechanical alloying and plasma activated sintering. A preferentially orientated microstructure with the basal planes (0 0 *l*) perpendicular to the pressing direction was formed, and the orientation factors of the (0 0 *l*) planes of the $Bi_{0.5}Sb_{1.5}Te_3$ and $Bi_{0.4}Sb_{1.6}Te_3$ alloys were 0.12 and 0.11, respectively. Effect of excess Te content on the thermoelectric properties of the $(Bi,Sb)_2Te_3$ alloys was investigated and the figure of merit of the $Bi_{0.4}Sb_{1.6}Te_3$ alloys decreased from 5.26×10^{-3} to $4.44 \times 10^{-3}\,K^{-1}$ with increasing the amount of excess Te to 8 wt.%, this should be ascribed to the fact that the chemical composition of the δ matrix phase displayed indifference with varying excess Te content and the presence of free Te second phase.

Keywords: Thermoelectric properties; $(Bi,Sb)_2Te_3$; Mechanical alloying; Plasma activated sintering

1. Introduction

In recent years, a broad search has been performed to develop new materials with high thermoelectric properties, including filled skutterudite [1], zinc antimonide [2], half Heusler [3], $AgPb_mSbTe_{2+m}$ [4], metal oxide [5], etc. Bismuth telluride based compounds is known as one of the most excellent thermoelectric materials around room temperature [6–9]. However, the thermoelectric properties of bulk Bi_2Te_3 based materials had not been improved obviously and the dimensionless figure of merit (*ZT*) was approximately 1 for many years. Although it is acceptable for some specialized applications, it is far less for commercial refrigeration in a large scale.

Most investigations were focused on optimizing the composition of Bi_2Te_3 based compounds, tuning doping with other heavy metals and optimizing device design. It is well known that the thermoelectric properties of p-type single crystal $(Bi,Sb)_2Te_3$ can be improved by doping excess Te to compensate the anti-structure defects and improved the carrier concentration [10]. However, there was uncertain about the effect of excess Te addition on the thermoelectric properties of polycrystalline $(Bi,Sb)_2Te_3$ prepared by powder metallurgical methods. One opinion was that the charge carrier content of p-type $(Bi,Sb)_2Te_3$ could be optimized by doping excess Te and thus improve the thermoelectric figure of merit (*Z*). For instance, the highest *Z* was obtained as $2.69 \times 10^{-3}\,K^{-1}$ for the hot pressed (HP) p-type $Bi_{0.5}Sb_{1.5}Te_3$ doped with excess 4 wt.% Te by Seo et al. [11]. Park et al. [12] reported the maximum *Z* of $2.78 \times 10^{-3}\,K^{-1}$ was obtained at room temperature for the hot extruded (HE) p-type $Bi_{0.5}Sb_{1.5}Te_3$ doped with 4.0 wt.% Te. Jiang et al. [7] obtained the maximum *Z* of $3.29 \times 10^{-3}\,K^{-1}$ at 350 K for the spark plasma sintered (SPS) p-type $Bi_{0.4}Sb_{1.6}Te_3$ by doping excess 3 wt.% Te. The other point of view was that the thermoelectric properties of p-type $(Bi,Sb)_2Te_3$ prepared by powder metallurgical methods could not be improved by doping excess Te. For instance, Hyun et al. [10] reported that the thermoelectric properties of the as-HPed 20% Bi_2Te_3–80% Sb_2Te_3 alloys showed inconspicuous dependence on the excess Te addition amount and the figure of merit held a line ($3.2 \times 10^{-3}\,K^{-1}$) regardless of the excess Te amount up to 10 wt.%. Shin et al. [13] also thought that the doping Te could not be adopted for the HP method.

* Corresponding author. Tel.: +86 27 87540944; fax: +86 27 87543776.
E-mail address: jyyang@public.wh.hb.cn (J. Yang).

0925-8388/$ – see front matter © 2006 Elsevier B.V. All rights reserved.
doi:10.1016/j.jallcom.2006.10.062

To clarify further the relationship between Te doping and the thermoelectric properties of $(Bi,Sb)_2Te_3$ compounds in mechanical alloying (MA) and subsequently plasma activated sintering (PAS) process. $(Bi,Sb)_2Te_3$ alloys with different amount of excess Te addition were prepared by MA and PAS in this paper, effect of excess Te amount on the thermoelectric properties of p-type $(Bi,Sb)_2Te_3$ alloys was investigated.

2. Experimental

Elemental Bi (99.99 wt.%, 200 mesh), Sb (99.99 wt.%, 100 mesh) and Te (99.99 wt.%, 100 mesh) powders were weighed according to an atomic ratio of $Bi_{0.4}Sb_{1.6}Te_3$ and $Bi_{0.5}Sb_{1.5}Te_3$, doped with excess x wt.% Te ($x = 0$, 2, 4, 6 and 8), and then subjected to MA in a planetary ball mill for 12 h in a high purified argon atmosphere. To minimize oxygen contamination, all powders weighing, loading and unloading were operated in a glove-box under a high purified argon atmosphere. Subsequently, the as-MAed powders were sintered by PAS under an axial compressive stress of 40 MPa at 410 °C for 20 min in an argon atmosphere and more details concerning to choosing the conditions of sintering were reported in our previous work [14]. Microstructure observation was performed with a field emission scanning electron microscope (Sirion 200) (FE-SEM). Phase identification and crystal orientation were analyzed with X-ray diffraction (XRD) in a Philips X'Pert PRO diffractometer by using Cu Kα radiation ($\lambda = 1.5406$ Å). Differential thermal analysis (DTA) was performed at a heating rate of 20 °C/min with a Perkin-Elmer DTA 7 differential thermal analyzer. Thermoelectric properties were measured at room temperature (27 °C) along to the section perpendicular to the pressing direction. A 10 °C temperature gradient was applied between two ends of a bar specimen (3 mm × 3 mm × 15 mm) to evaluate Seebeck coefficient (α). Electrical resistivity (ρ) was measured by a four-probe method. A laser flash apparatus (ULVAC-RIKO, TC-7000) was employed for thermal diffusivity and specific heat measurement, thermal conductivity was calculated from the values of thermal diffusivity, specific heat and density.

3. Results and discussion

SEM fractographs of the as-PASed $Bi_{0.4}Sb_{1.6}Te_3$ (a) and $Bi_{0.5}Sb_{1.5}Te_3$ (b) alloys from sections perpendicular to the pressing direction are shown in Fig. 1. Homogeneous microstructure and plate grains can be observed. The grain size is about 0.5–0.8 μm, which is much smaller than that of Bi_2Te_3 based alloys by the other methods such as HP (2 μm) [7], HE (5 μm) [8] and zone-melting (>50 μm) [7], which would enhance phonon-grain boundary scattering and decrease lattice thermal conductivity.

Fig. 2 shows XRD patterns of the as-PASed $Bi_{0.4}Sb_{1.6}Te_3$ (a) and $Bi_{0.5}Sb_{1.5}Te_3$ (b) billets from sections parallel and perpendicular to the pressing direction. All the as-milled powder and the as-PASed billets show a single phase $(Bi,Sb)_2Te_3$ structure and impurities cannot be found. Furthermore, XRD peaks of the as-PASed $(Bi,Sb)_2Te_3$ solid solution become sharper and stronger after PAS, indicating the improvement of crystallinity and release of crystalline defects and remnant stress resulted from MA process after PAS. The relative intensities of (0 0 l) planes including (0 0 6), (0 0 15), (0 0 9) and (0 0 18) from sections perpendicular to the pressing direction are lightly stronger than those from sections parallel to the pressing direction, indicating that the basal planes are preferentially orientated perpendicular to pressing direction. The orientation degree of the (0 0 l) planes can be determined by the orientation factor F, which can

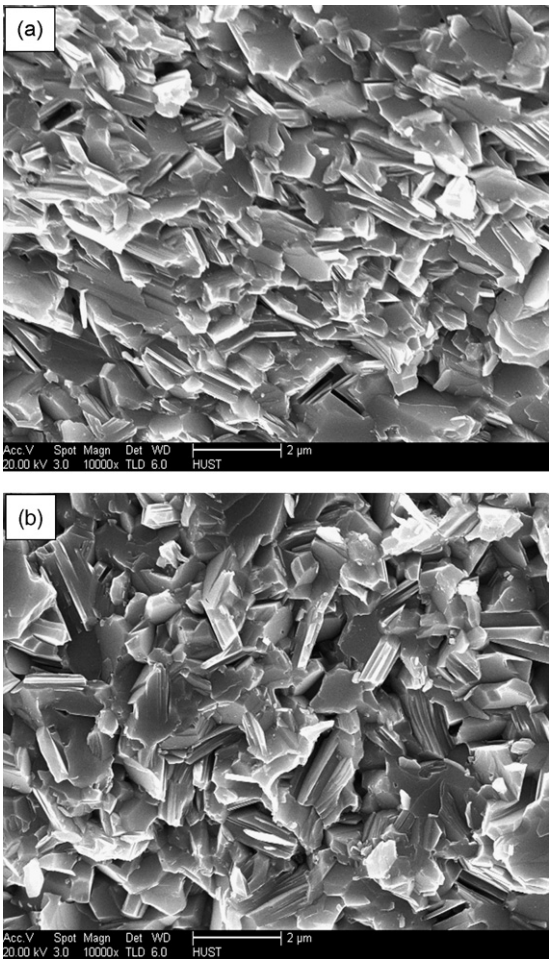

Fig. 1. SEM fractographs of the sintered $Bi_{0.4}Sb_{1.6}Te_3$ (a) and $Bi_{0.5}Sb_{1.5}Te_3$ (b) billets from sections perpendicular to the pressing direction.

be calculated using Lotgering method [15]:

$$F = \frac{P - P_0}{1 - P_0}, \quad P = \frac{I(0\,0\,l)}{\sum I(h\,k\,l)}, \quad P_0 = \frac{I_0(0\,0\,l)}{\sum I_0(h\,k\,l)}$$

where P and P_0 are the ratios of the integrated intensities of all (0 0 l) planes to those of all (h k l) planes for the preferentially orientated and randomly orientated samples, respectively. The orientation factors F of the (0 0 l) planes of the PASed $Bi_{0.5}Sb_{1.5}Te_3$ and $Bi_{0.4}Sb_{1.6}Te_3$ billets are 0.12 and 0.11, respectively. The preferential orientation formation is mainly attributed to the lamellar crystal structure and the weak van der Waals bonding between $Te^{(1)}$ and $Te^{(1)}$ [7]. The particles with basal planes bonded by van der Waals force would rotate perpendicular to the pressing direction. Furthermore, the pulse current induced a high electric field in samples and might promote the preferential orientation [14,16].

Typical DTA curve of the as-PASed $Bi_{0.4}Sb_{1.6}Te_3$ alloy is presented in Fig. 3. The endothermic peak near 420 °C corresponds to the formation of Te-rich eutectic liquid phase, and the larger endothermic peak at about 620 °C corresponds to the melting of $Bi_{0.4}Sb_{1.6}Te_3$ solid solution. According to the DTA result and the micro-phase diagram near the stoichiometric composition of $Bi_{0.4}Sb_{1.6}Te_3$ [10], it can be known that the equilibrium

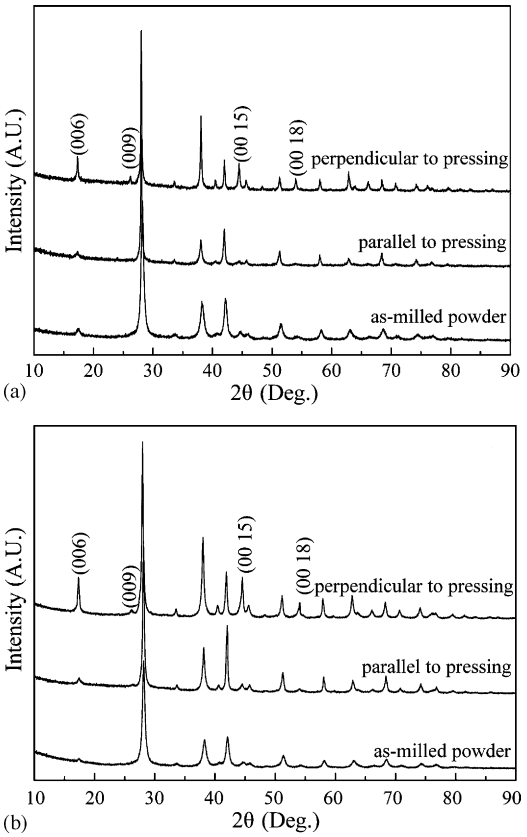

Fig. 2. XRD patterns of the sintered $Bi_{0.4}Sb_{1.6}Te_3$ (a) and $Bi_{0.5}Sb_{1.5}Te_3$ (b) alloys from sections parallel and perpendicular to the pressing direction.

microstructure phase of the $Bi_{0.4}Sb_{1.6}Te_3$ solid solution is δ + Te when temperature is below 420 °C, and liquid + δ when temperature is between 420 and 620 °C.

Electrical resistivity (ρ) and Seebeck coefficient (α) of the as-PASed $Bi_{0.5}Sb_{1.5}Te_3$ and $Bi_{0.4}Sb_{1.6}Te_3$ alloys as a function of excess Te amount are shown in Fig. 4 and Fig. 5, respectively. The electrical resistivity increases lightly with increasing excess Te content up to 4 wt.%, and then fluctuates lightly when the amount of doping Te varies from 4 to 8 wt.%. When the $(Bi,Sb)_2Te_3$ powders with different amounts of excess Te addition are sintered at 410 °C, the molar ratio of δ-phase and free Te second phase will be changed according to the level rule in the

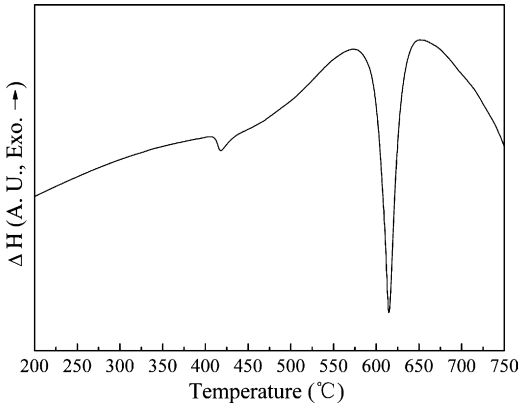

Fig. 3. DTA curve of the sintered $Bi_{0.4}Sb_{1.6}Te_3$ alloy.

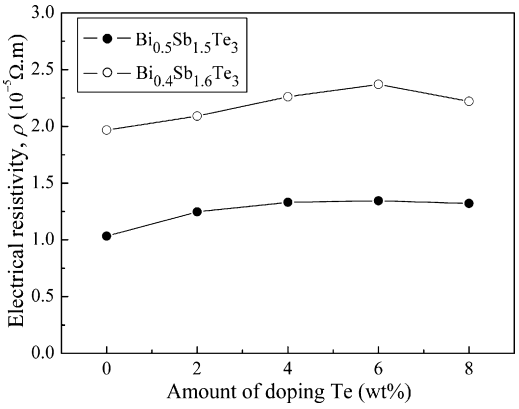

Fig. 4. Amount of excess Te addition dependence of electrical resistivity (ρ) of the sintered $Bi_{0.5}Sb_{1.5}Te_3$ and $Bi_{0.4}Sb_{1.6}Te_3$ alloys.

micro-phase diagram. However, the chemical composition of the δ-phase is identical regardless of the excess Te amount according to micro-phase diagram near the stoichiometric composition of $Bi_{0.4}Sb_{1.6}Te_3$ solid solution [10]. Even with tuning the amount of excess Te up to 8 wt.%, the PASed $Bi_{0.4}Sb_{1.6}Te_3$ are composed of δ matrix phase with the same chemical composition and a small amount of free Te second phase. Therefore, a majority of excess Te will not be reacted into the master alloys, and the Te second phase distributes near crystal boundary, which will enhance the scattering of carrier, decrease mobility and result in the increasing of electrical resistivity. Seebeck coefficient is almost unchanged regardless of the excess Te amount (Fig. 5). As we know, at a constant temperature T, Seebeck coefficient can be simplified as [11]:

$$\alpha = \frac{k_B}{e}(\delta + C - \ln n_c),$$

where n_c is the carrier concentration; k_B the Boltzmann constant; δ is the scattering parameter. Even with tuning the amount of excess Te up to 8 wt.%, the PASed $Bi_{0.4}Sb_{1.6}Te_3$ are composed of δ matrix phase with the same chemical composition, and it can be reasonably surmised that the excess Te cannot compensate the anti-structure defects and adjust carrier concentration. Therefore, Seebeck coefficient cannot be changed by tuning the amount of excess Te.

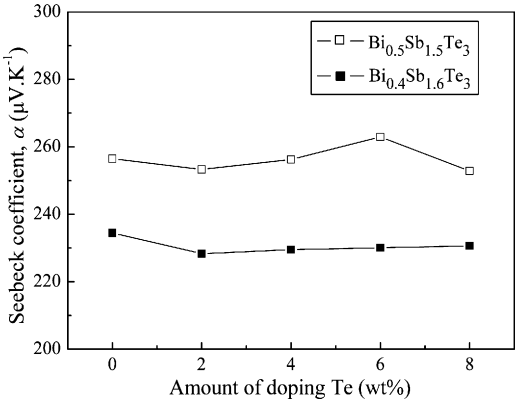

Fig. 5. Amount of excess Te addition dependence of Seebeck coefficient (α) of the sintered $Bi_{0.5}Sb_{1.5}Te_3$ and $Bi_{0.4}Sb_{1.6}Te_3$ alloys.

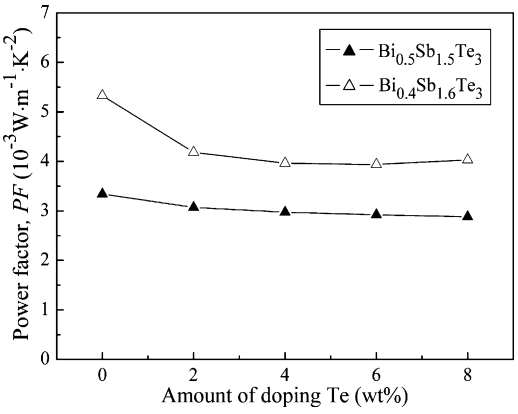

Fig. 6. Amount of excess Te addition dependence of power factor (PF) of the sintered $Bi_{0.5}Sb_{1.5}Te_3$ and $Bi_{0.4}Sb_{1.6}Te_3$ alloys.

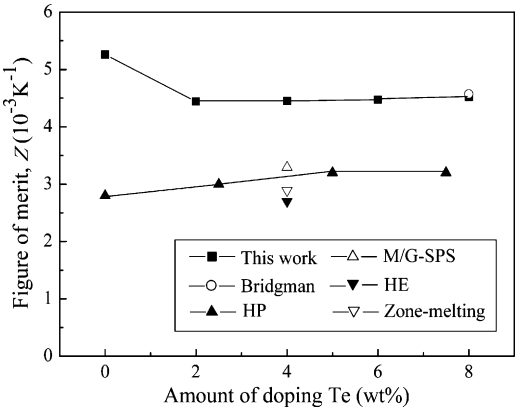

Fig. 8. Amount of excess Te addition dependence of figure of merit (Z) of the sintered $Bi_{0.4}Sb_{1.6}Te_3$ alloys.

Fig. 6 presents the variation of power factor (PF) of the as-PASed $Bi_{0.5}Sb_{1.5}Te_3$ and $Bi_{0.4}Sb_{1.6}Te_3$ alloys with amount of excess Te addition. It is clear that the power factor is deteriorated by doping excess Te, which should result from the increase of electrical resistivity (ρ).

Fig. 7 displays the amount of excess Te addition dependence of thermal conductivity (κ) of the as-PASed $Bi_{0.4}Sb_{1.6}Te_3$ alloys. The total thermal conductivity decreases lightly from 1.013 to 0.890 $W\,m^{-1}\,K^{-1}$ when increasing excess Te amount up to 4 wt.%, and then fluctuates near 0.900 $W\,m^{-1}\,K^{-1}$ when further increasing excess Te content up to 8 wt.%. As we know, thermal conductivity of semiconductor can be approximately expressed as [17]:

$$\kappa = \kappa_{el} + \kappa_{ph},$$

where κ_{el} and κ_{ph} correspond to carrier and phonon contribution to thermal conductivity, respectively. The carrier-related thermal conductivity κ_{el} can be calculated from the electrical resistivity (ρ) according to the Wiedemann–Franz law [17]:

$$\kappa_{el} = \frac{LT}{\rho},$$

where L is the Lorentz constant. The carrier-related thermal conductivity κ_{el} decrease from 0.712 to 0.552 $W\,m^{-1}\,K^{-1}$ when increasing excess Te amount to 4 wt.%, which should be attributed to the enhancement of the scattering of carrier due to the presence of the free second Te phase. However, the phonon contribution to thermal conductivity κ_{ph} shows indifference with increasing the amount of excess Te. The lattice thermal conductivity is mainly determined by the lattice vibration and it is relevant with the microstructure and component of materials. On one hand, the excess Te at grain boundary results in no anti-site defect or lattice distortion in the $(Bi,Sb)_2Te_3$ solid solution phase, therefore, it makes no influence to the lattice vibration; on the other hand, even if the excess Te is precipitated near grain boundary, the effect of a small amount of excess interface on phonon scattering, which comes from the excess Te, can be ignored in comparison with the large amounts of grain boundary. So the lattice thermal conductivity is almost independent of the excess Te content.

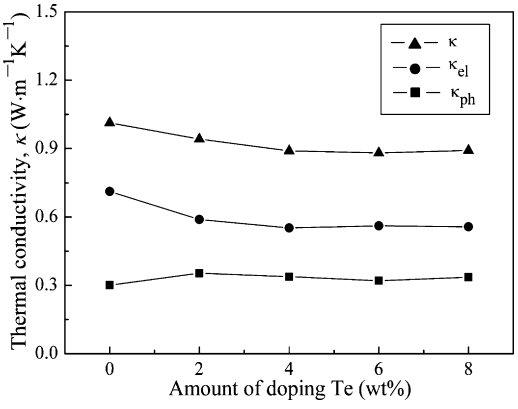

Fig. 7. Amount of excess Te addition dependence of thermal conductivity (κ) of the sintered $Bi_{0.4}Sb_{1.6}Te_3$ alloys.

The figure of merit of the as-PASed $Bi_{0.4}Sb_{1.6}Te_3$ alloys are shown in Fig. 8 as a function of the amount of excess Te addition, and the results for those materials prepared by HP [10], HE [18], melting/grinding-spark plasma sintering (M/G-SPS) [7], Bridgman [6] and zone melting [7] methods are also presented for comparison. Because of very lightly decrease of thermal conductivity with excess Te addition (Fig. 7), the figure of merit shows almost the same trend as the power factor (Fig. 6) for $Bi_{0.4}Sb_{1.6}Te_3$ alloys doped with different amount of excess Te. The figure of merit of the MA-PASed $Bi_{0.4}Sb_{1.6}Te_3$ alloys decreases from 5.26×10^{-3} to $4.44 \times 10^{-3}\,K^{-1}$ with increasing the amount of excess Te up to 2 wt.% and almost holds a line when further increasing excess Te content up to 8 wt.%. Although the figure of merit is deteriorated by doping excess Te, it is still significantly higher than those of the alloys prepared via HP [10], HE [18], M/G-SPS [7], Bridgman [6] and zone melting [7] methods.

There are several factors that may cause the improvement of the thermoelectric properties of p-type $(Bi,Sb)_2Te_3$ alloys prepared by MA-PAS process. (1) MA can obtain powders with very fine microstructure. (2) During the PAS process, plasma is generated due to discharge between powders and the oxidation layer on the surface of powders is destroyed and the powders are purified. So the PASed samples keep high carrier

mobility and result in decrease of electrical resistivity. The carrier mobility of the MA-PASed $Bi_{0.5}Sb_{1.5}Te_3$ and $Bi_{0.4}Sb_{1.6}Te_3$ samples are 262.0 and 287.8 $cm^2\ V^{-1}\ s^{-1}$ in this work, respectively. Min et al. [19] reported that the carrier mobility of the HEed $Bi_{0.5}Sb_{1.5}Te_3$ was 108 $cm^2\ V^{-1}\ s^{-1}$ and Yang et al. [20] reported that the carrier mobility of the HPed $Bi_{0.5}Sb_{1.5}Te_3$ alloy was 175 $cm^2\ V^{-1}\ s^{-1}$. As to the M/G-SPSed samples, the very large carrier mobility (866 $cm^2\ V^{-1}\ s^{-1}$) was obtained by Jiang et al. [7]. It is obviously higher than our PASed samples, which should be ascribed to the large grain size (>50 μm). The grain size in our work is only 0.5–0.8 μm. (3) The surface of powders is activated by plasma and a self-heating phenomenon is achieved between the particles, heat-transfer and mass-transfer can be completed instantaneously. Therefore, it can obtain materials with very fine microstructure and high density (>99% T.D.) at a relatively lower sintering temperature (410 °C) and in a very short time (20 min), which should be helpful to enhance phonon-grain boundary scattering and reduce phonon thermal conductivity. (4) The lower sintering temperature and shorter sintering time are helpful to avoid over-evaporation of some elements and keep good homogeneity of composition and thus improve the electrical properties.

It is well known that the chemical compositions of the unidirectionally grown samples will change along the solid line and the δ-phase becomes less Te deficient according to micro-phase diagram near the stoichiometric composition of $Bi_{0.4}Sb_{1.6}Te_3$ solid solution, therefore, excess Te can be added into the single crystal to occupy its own site to compensate the anti-structure defects and optimize the charge carrier concentration [10]. However, the thermoelectric properties of the MA-PASed $(Bi,Sb)_2Te_3$ compounds cannot be controlled with variation of the amount of excess Te addition. Different from some conventional preparing methods, MA-PAS process includes MA and PAS two consecutive processes, in which MA process is performed at room temperature, element powders directly react into the matrix phase by solid phase reaction, which would be different from the phase transformation during the melting-solidifying process; on the other hand, PAS process is performed at a relatively lower sintering temperature and in a much shorter time than those of conventional methods, such as unidirectional solidification, HP or HE. It is probable that the phase and its composition, microstructure and atomic local environment in the as-PASed Bi_2Te_3 based alloys would be different from the case of the single crystals and the as-HPed or the as-HEed polycrystalline materials. Although the molar ratio of δ-phase and free Te second phase can be changed according to the level rule, the chemical compositions of the δ matrix phase cannot be changed during PAS process. So the thermoelectric properties of the MA-PASed $(Bi,Sb)_2Te_3$ materials cannot be optimized by excess Te doping to adjust carrier concentration regardless of the excess Te amount up to 8 wt.%.

4. Conclusions

The p-type Te-doped $(Bi,Sb)_2Te_3$ alloys are prepared by MA-PAS. A preferentially orientated microstructure with the basal planes (0 0 *l*) perpendicular to the pressing direction is formed, and the orientation factors of the (0 0 *l*) planes of the as-PASed $Bi_{0.5}Sb_{1.5}Te_3$ and $Bi_{0.4}Sb_{1.6}Te_3$ alloys are 0.12 and 0.11, respectively. Although the power factor is 26% lower than the undoped-$Bi_{0.4}Sb_{1.6}Te_3$ compounds and the figure of merit (Z) decreases from 5.26×10^{-3} to $4.44 \times 10^{-3}\ K^{-1}$ with excess Te addition, it is still significantly higher than those of the alloys prepared via HP, HE, M/G-SPS, zone melting and Bridgman methods.

Acknowledgements

This work is co-financed by the Nation Basic Research Project (2004CCA03200) and Natural Science Foundation of China (50401008).

References

[1] C. Uher, Semiconduct. Semimet. 69 (2001) 139–253.
[2] T. Caillat, J.P. Fleurial, A. Borshchevsky, J. Phys. Chem. Solids 58 (1997) 1119–1125.
[3] S.J. Poon, Semiconduct. Semimet. 70 (2001) 37–75.
[4] K.F. Hsu, S. Loo, F. Guo, W. Chen, J.S. Dyck, C. Uher, T. Hogan, E.K. Polychroniadis, M.G. Kanatzidis, Science 30 (2004) 818–821.
[5] H. Muta, K. Kurosaki, S. Yamanaka, J. Alloy. Compd. 368 (2004) 22–24.
[6] O. Yamashita, S. Tomiyoshi, J. Appl. Phys. 93 (2003) 368–374.
[7] J. Jiang, L.D. Chen, S.Q. Bai, Q. Yao, Q. Wang, Scripta Mater. 52 (2005) 347–351.
[8] S.J. Hong, B.S. Chun, Mater. Sci. Eng. A 356 (2003) 345–361.
[9] D.Y. Chung, T. Hogan, P. Brazis, M.R. Lane, C. Kannewurf, M. Bastea, C. Uher, M.G. Kanatzidis, Science 287 (2000) 1024–1027.
[10] D.B. Hyun, T.S. Oh, J.S. Hwang, J.D. Shim, Scripta Mater. 44 (2001) 455–460.
[11] J. Seo, K. Park, D. Lee, C. Lee, Scripta Mater. 38 (1998) 477–484.
[12] K. Park, J. Seo, D.C. Cho, B.H. Choi, C.H. Lee, Mater. Sci. Eng. B 88 (2002) 103–106.
[13] H.S. Shin, H.P. Ha, D.B. Hyun, J.D. Shim, D.H. Lee, J. Phys. Chem. Solids 58 (1997) 671–678.
[14] X.A. Fan, J.Y. Yang, R.G. Chen, H.S. Yun, W. Zhu, S.Q. Bao, X.K. Duan, J. Phys. D Appl. Phys. 39 (2006) 740–745.
[15] F.K. Lotgering, J. Inorg. Nucl. Chem. 9 (1959) 113–116.
[16] X.A. Fan, J.Y. Yang, W. Zhu, H.S. Yun, R.G. Chen, S.Q. Bao, X.K. Duan, J. Alloy. Compd. 420 (2006) 256–259.
[17] J.Y. Yang, X.A. Fan, R.G. Chen, W. Zhu, S.Q. Bao, X.K. Duan, J. Alloy. Compd. 416 (2006) 270–273.
[18] J. Seo, D. Cho, K. Park, C. Lee, Mater. Res. Bull. 35 (2000) 2157–2163.
[19] B.G. Min, K.W. Jang, D.B. Hyun, D.H. Lee, Proceedings of the 16th International Conference on Thermoelectrics (IEEE), Dresden, Germany, 1997, pp. 76–80.
[20] J. Yang, T. Aizawa, A. Yamamoto, T. Oht, Mater. Chem. Phys. 70 (2001) 90–94.